

# A mechanism for magnetic field stochastization and energy release during an edge pedestal collapse

T. Rhee, S. S. Kim, Hogun Jhang,\* G. Y. Park, and R. Singh

*National Fusion Research Institute,  
Daejeon 305-333, Republic of Korea*

## Abstract

On the basis of three-dimensional nonlinear magnetohydrodynamic simulations, we propose a new dynamical process leading to the stochastization of magnetic fields during an edge pedestal collapse. Primary tearing modes are shown to grow by extracting kinetic energy of unstable ballooning modes, eventually leading to the island overlap. Secondary tearing modes, which are generated through a coherent nonlinear interaction between adjacent ballooning modes, play a key role in this process, mediating the energy transfer between primary ballooning and tearing modes. Explicit calculations of the parallel energy loss through the stochastic field lines show that it can be a likely dominant energy loss mechanism during an edge pedestal collapse.

PACS numbers: 05.45.-a, 52.25.Gj, 52.35.Mw, 52.35.Py

Keywords: Nonlinear, Tearing modes, Stochastic fields, Collisionless diffusion

An edge localized mode (ELM) is an instability occurring in the edge pedestal region of magnetic fusion plasmas. It is, in some sense, an unavoidable consequence of operating a plasma in an enhanced edge confinement mode, *i.e.* the H-mode [1], characterized by a steep pressure gradient. Large ELMs are accompanied with unacceptably high heat flux to divertor and plasma facing materials in fusion devices. Therefore, elucidating physics mechanisms responsible for the ELM crash and ensuing energy losses has been a central issue for decades in contemporary plasma physics, as an effort to avoid or mitigate ELMs.

The present idea on the origin of ELMs is based on the destabilization of ideal peeling-ballooning modes [2]. Formation and ejection of filamentary structures have been observed in both nonlinear MHD simulations [3–5] and experiments [6–10] during ELM crashes. Thus, ELMs have often been associated with these filamentary structures. A theory has been proposed on the origin of the filamentary structure based on nonlinear evolution of the ballooning mode [11]. However, a recent study shows that the energy loss due to the filaments is estimated to be  $\lesssim 30\%$  of the total energy loss [12]. Then, the identification of the physical mechanism accounting for  $\gtrsim 70\%$  of the ELM energy loss remains as a question.

Nonlinear MHD and gyrofluid simulations have often shown the generation of stochastic magnetic fields during a simulated edge pedestal collapse, though the degree of stochastization varies in models being applied [3, 5, 13, 14]. Since the triggering instabilities of ELMs are ballooning modes possessing the twisting parity in nature, it is a puzzle how these stochastic field lines are generated out of the initial ballooning modes. Some nonlinear mechanisms have been invoked to explain the generation of stochastic fields. However, no detailed analysis shedding light on the process of stochastization is yet available. In this Letter, we elucidate, on the basis of three-dimensional nonlinear reduced MHD simulations, a mechanism leading to the magnetic field stochastization during an edge pedestal collapse. Development of a series of nonlinearly driven tearing modes and ensuing island overlap are shown to be responsible for the generation of stochastic magnetic fields. In particular, we highlight the role of the secondary tearing mode, which is generated via a coherent nonlinear interaction between adjacent ballooning modes, as an *agent* for the energy transfer from the unstable ballooning mode to the primary tearing mode. We also show that the collisionless parallel energy transport through the stochastic field lines can be a main energy

loss mechanism during the crash.

We perform edge pedestal collapse simulations using a three-field reduced MHD model, which consists of evolution equations for vorticity and pressure, and Ohm's law. The computational model is basically the same as that of previous studies [14–16], except for the pressure evolution equation, as will be described later. All simulations are performed by using the BOUT++ framework [17] without sources and sinks. Basic parameters in the simulation are as follows:  $R_0 = 3.5$  (m) is the major radius,  $V_A = 9.5 \times 10^6$  (m/sec) the Alfvén velocity,  $S = \mu_0 R_0 V_A / \eta = 10^9$  the Lundquist number, and  $S_H = \mu_0 R_0^3 v_A / \eta_H = 10^{12}$  the hyper-Lundquist number. The computational domain is  $-0.6 \leq \psi_N \leq 0.2$ , where  $\psi_N$  is the normalized poloidal flux with  $\psi_N = 0$  corresponding to the location of the approximate last closed flux surface. A monotonic  $q$ -profile in the range,  $1.19 \leq q \leq 4.87$  with  $0.66 \leq s = (r/q)(dq/dr) \leq 6.26$  is used.  $q$  and  $s$  values at the maximum pressure gradient location ( $r_{max}$ ) are 2.1 and 4.35, respectively. The normalized pressure profile  $\alpha = -2\mu_0 q^2 R_0 (dP_0/dr) / B^2 = 3.86$  at  $r = r_{max}$  while the critical  $\alpha$  is  $\alpha_c = 2.75$ . Thus, the initial pressure profile is unstable to the peeling-ballooning mode. Simulations can be performed using different initial perturbations. A recent study emphasizes the role of initially unstable multi-modes in pedestal collapse [16]. In this Letter, we present results initiated from an unstable single mode because it clearly reveals the nonlinear physics process leading to magnetic reconnection. We have found that multi-mode simulations yield almost identical results and conclusions presented in this Letter, as long as the initial energy of the unstable ballooning mode is strong enough.

Figure 1(a) shows the field line trace at  $t = 50 \tau_A$  ( $\tau_A$ : Alfvén time), which typifies a stage just prior to stochastization, in the toroidal ( $Z$ , normalized to 1) and radial ( $X = \psi_N$ ) plane. Hereafter, we use  $\tau_A$  as a unit of time throughout. An interesting observation can be made in Fig. 1(b) where field lines corresponding to  $n = 2n_0$  ( $n_0$ : toroidal mode number of the most unstable ballooning mode) are shown at  $t = 55$ . One can see the growth of magnetic islands, in the middle of two flux surfaces (dotted line) where the ballooning modes are most unstable (two solid lines). We designate these as the *secondary tearing modes* (STM). Figure 1(c) shows the spatio-temporal evolution of the Chirikov parameter ( $C$ ) during a simulation. The contour for  $C = 1$  (the thick black line) indicates that the stochastization initiates from  $t \approx 60$  at just inside the separatrix where the ballooning mode is most unstable, propagates almost linearly into the core, and saturates (*i.e.*, ceases to

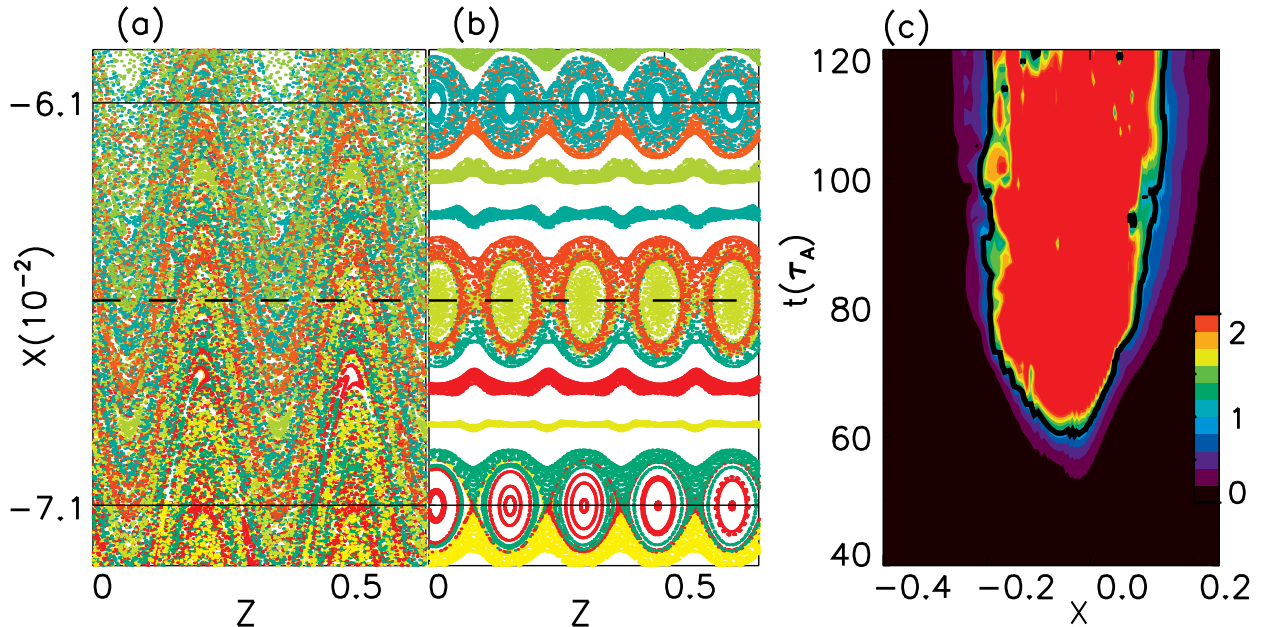


FIG. 1. Field line traces at  $t = 50 \tau_A$  ( $\tau_A$ : Alfvén time) (a) and  $t = 55 \tau_A$  corresponding to  $2n_0$  ( $n_0$ : the toroidal mode number of the most unstable ballooning mode) (b) in the toroidal ( $Z$ , normalized to 1) and radial ( $X = \psi_N$ ) plane. The dotted line represents the midpoint between two flux surfaces where the ballooning modes are most unstable (two solid lines). (c) Spatio-temporal evolution of the Chirikov parameter.

propagate) at  $t \approx 75$ . Stochastization of magnetic fields after  $t \gtrsim 60$  is shown to be mainly due to the growth of tearing modes with the *same* mode number as the initial ballooning modes. We designate these tearing modes and initial ballooning modes as *primary tearing modes* (PTM) and *primary ballooning modes* (PBM), respectively.

A question then arises as to how the even parity tearing modes (STMs and PTMs) are generated from the odd parity PBMs. The ballooning instabilities are known to be difficult to generate magnetic reconnection due to their nonlinear self-acceleration property [18]. The generation of even parity modes can be seen more clearly in Fig. 2(a) where the volume-integrated intensity for the total even ( $\psi^+$ , red) and odd ( $\psi^-$ , blue) components of the perturbed flux ( $\psi$ ),  $\int_V |\psi^\pm|^2 dV$ , are plotted as a function of time. Even parity modes start to grow rapidly around  $t \sim 60$ , saturates for  $70 \lesssim t \lesssim 85$ , then reduces to a steady state value at  $t \sim 105$ . At final stage,  $\int_V |\psi^+|^2 dV \simeq \int_V |\psi^-|^2 dV$ , implying the equipartition of magnetic energy between even and odd parity modes.

Figure 2(b) shows the time evolution of volume-integrated amplitudes for the most unsta-

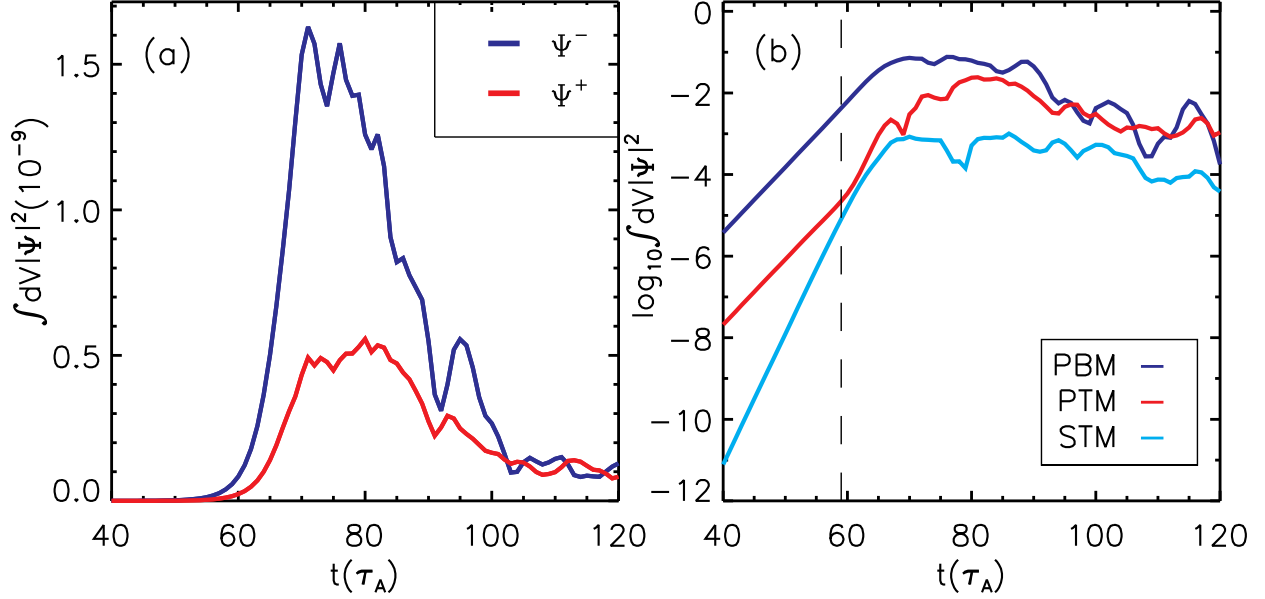


FIG. 2. Time evolution of volume-integrated intensity for (a) odd (blue) and even (red) parity modes and (b) PBM (blue), PTM (red), and STM (cyan).

ble PBM (blue), PTM (red) and the corresponding STM (cyan). In a linear stage ( $t \lesssim 60$ ), both PBM and PTM co-exist and grow with the same growth rate, even though the magnitude of PBM is dominant. The initial even parity mode is parasitic and irrelevant to the actual tearing mode growth. The growth rate of STM is exactly twice that of primary modes, as will be shown shortly. We emphasize that this STM is a nonlinearly driven mode which grows even when  $\Delta'_{STM} \equiv [(1/\psi_{STM})(d\psi_{STM}/dr)]_{-W_s/2}^{W_s/2} < 0$ , where  $W_s$  is the island width of the STM. When the magnitude of STM becomes comparable to that of PTM at  $t \simeq 60$ , the growth of PTM is accelerated. This acceleration is shown to be possible only mediated by STM. Finally, PTMs give rise to an island overlap and subsequent field line stochastization. These observations suggest that magnetic reconnection and ensuing field line stochastization involves a strong nonlinear interaction among PBM, PTM and STM.

To study the nonlinear interaction quantitatively, we first evaluate time evolution of growth rates for PBM ( $\gamma_0^-$ ), PTM ( $\gamma_0^+$ ) and STM ( $\gamma_2^+$ ), the results of which are shown in Fig. 3(a). One can see that  $\gamma_2^+ = 2\gamma_0^-$ , implying the STM is driven by a coherent nonlinear interaction between adjacent PBMs. The beating of adjacent PBMs with the mode numbers  $(m_0, n_0)$  and  $(m_0 + 1, n_0)$  generates a STM with the mode number  $(2m_0 + 1, 2n_0)$ . Also, one can observe that a sudden increase of  $\gamma_0^+$  around  $t \approx 60$  is synchronized to the drop of

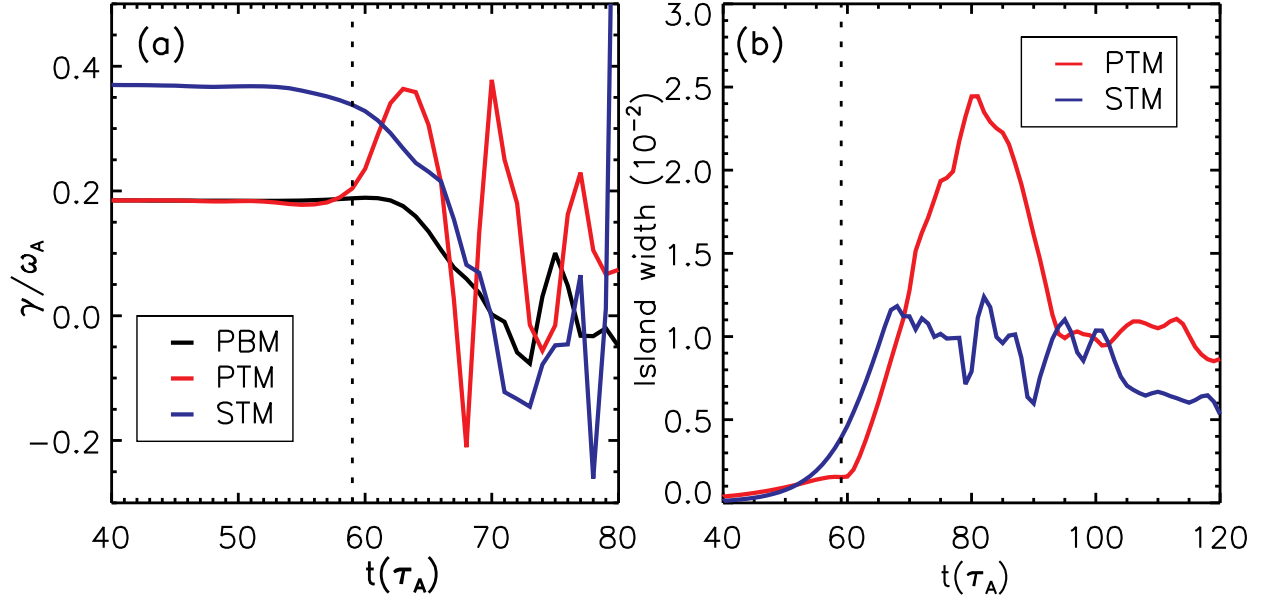


FIG. 3. Time evolution of (a) growth rates for PBM, PTM and STM, and (b) island width corresponding to STM (blue) and PTM (red).

$\gamma_2^+$ . This signifies the weakening of STM growth due to the growth of PTM. Figure 3(b) shows time evolution of the island width corresponding to STM (blue,  $W_s$ ) and PTM (red,  $W_p$ ).  $W_s$  grows first and approaches to the inter-surface distance,  $W_s \approx 1/n_0q'$ , at  $t \simeq 60$ . Then,  $W_p$  begins to grow rapidly. The initial stochastization of magnetic fields at this time are due to the island overlap by the STMs, while the full stochastization is realized by the PTMs after the initial stochastization. Thus, we arrive at a provisional conclusion that the nonlinear energy transfer among relevant modes are ultimately responsible for the generation of nonlinearly driven tearing modes and leads to the field line stochastization.

For a detailed study of this nonlinear energy transfer process, we evaluate the volume integrated nonlinear energy transfer rate to the magnetic energy of the  $(m_0, n_0)$  mode,

$$\Gamma_{m_0, n_0} = 2\text{Re} \sum_{m, n} \int_V J_{m_0, n_0}^+ [\phi_{m, n}, \psi_{m_0+m, n_0+n}^*] dV, \quad (1)$$

where  $J_{m_0, n_0}^+ = \nabla_{\perp}^2 \psi_{m_0, n_0}^+$ , and  $[a, b]$  denotes the conventional Poisson bracket operation.  $\Gamma_{m_0, n_0}$  represents how much energy is transferred to the  $(m_0, n_0)$  even parity mode from the kinetic energy of  $(m, n)$  mode represented by  $\phi_{m, n}$ . Thus, the PTM with the mode number  $(m_0, n_0)$  is predominantly generated through the coupling between the adjacent PBM and the STM represented by  $\phi_{m_0+1, n_0}$  and  $\psi_{2m_0+1, 2n_0}^*$ , respectively.

Figure 4(a) shows time evolution of  $\Gamma_{m_0, n_0}$  for STM (red solid) and PTM (black solid).  $\Gamma_{STM}$  starts to rapidly increase around  $t \simeq 60$  and reaches to its maximum value at  $t \simeq 70$ . Then,  $\Gamma_{PTM}$  starts to increase rapidly. The dotted line in Fig. 4(a) shows evolution for the normalized half-width of the magnetic island due to the STM,

$$C_{STM} = \frac{W_{2m_0+1, 2n_0}}{2(\psi_{2m_0+1, 2n_0} - \psi_{2m_0, 2n_0})}.$$

A strong energy transfer to PTM, which is represented by a sudden increase of  $\Gamma_{m_0, n_0}$  at  $t \simeq 70$ , occurs when the island due to STM approaches to the  $(m_0, n_0)$  flux surface, *i.e.*, when  $C_{STM} \simeq 1$ . Thus, PTM grows by extracting kinetic energy of an adjacent PBM *via* STM. We emphasize here the crucial role of STM as a *mediator* transferring the PBM kinetic energy to the magnetic energy of PTM, as depicted in Fig. 4(b) schematically. Without excitation of STM, PBM1 cannot directly deliver its energy to PTM at the location of PBM2. We note that this nonlinear energy transfer mechanism is, in some sense, akin to that of the vortex mode which was studied in Refs. [19] and [20] where nonlinear tearing mode generation is considered from a single primary mode. A major difference between the present work and Refs. [19] and [20] is that a STM is generated by two PBMs, not by one primary tearing mode as in the latter cases, and plays as an *agent* in the nonlinear energy transfer process delivering the kinetic energy of a PBM to the magnetic energy of an adjacent PTM.

Having identified the process leading to magnetic field stochasticization, we now consider collapse-induced energy losses when stochastic magnetic fields are present. To this end, we add a term representing heat conduction along the stochastic field lines ( $Q_{||}$ ) in the pressure evolution equation,

$$\frac{\partial P}{\partial t} + [\phi, P] = Q_{||}. \quad (2)$$

To find an appropriate model for  $Q_{||}$ , we first evaluate the ratio of Lyapunov length ( $L_c$ ) of a magnetic field to the collisional mean free path ( $l_{mfp}$ ) using the parameters in the simulation, giving rise to  $\lambda \equiv L_c/l_{mfp} \simeq 0.01$ , where  $L_c$  is evaluated numerically at  $t = 70$ . The whole stochasticization process takes place approximately within  $\sim 30 \tau_A$  corresponding to  $\sim 0.07 \tau_{ei}$  ( $\tau_{ei}$ : electron-ion collision time) in this simulation. The above two conditions indicate that the stochasticization process and ensuing energy losses should be dealt as a collisionless process.

An appropriate collisionless fluid model for  $Q_{||}$  in the presence of stochastic field lines is not available at present. From kinetic simulations, Park *et. al.* showed that the parallel

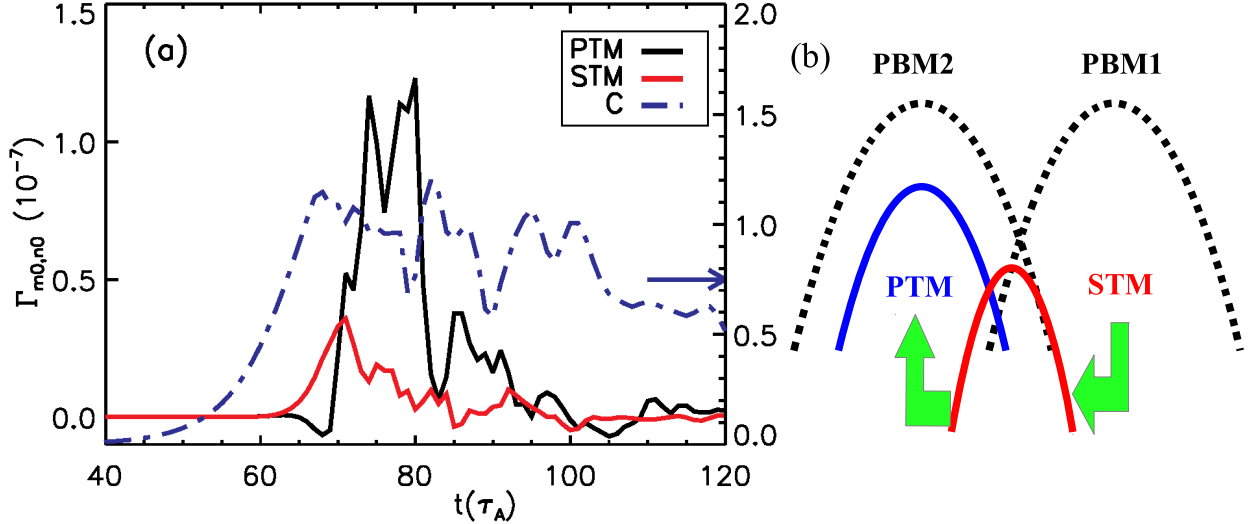


FIG. 4. (a) Time evolution of the volume integrated nonlinear energy transfer rate ( $\Gamma_{m_0, n_0}$ ) to the magnetic energy of STM (red) and PTM (black).  $\Gamma_{m_0, n_0}$  is defined in Eq. (1). The dotted line represents the normalized half-width of the magnetic island due to the STM. (b) A schematic diagram illustrating the energy transfer process from the kinetic energy of PBM1 to the magnetic energy of PTM at the location of PBM2 *via* STM.

electron heat conduction obeys the Rechester-Rosenbluth diffusion model [21] when one includes a factor accounting for kinetic effects [22]. Motivated by Ref. [22], we employ the collisionless Rechester-Rosenbluth model to evaluate  $Q_{\parallel}$

$$Q_{\parallel} = f_K v_e^2 D_{RR} \frac{\partial^2 \langle P \rangle}{\partial r^2}, \quad (3)$$

where  $\langle P \rangle$  is an equilibrium component of pressure and  $D_{RR} = \pi v_e R \sum_{m,n} (\delta B_{mn}/B_T)^2 \delta_{n,m/q}$  with  $v_e$  the electron thermal speed and  $\delta B_{mn}$  the perturbed radial magnetic field with the mode number  $(m, n)$ .  $f_K$  is a factor introduced to account for the reduction of thermal diffusion due to kinetic effects. The precise value of  $f_K$  is unknown. This will require a more sophisticated kinetic modelling or a fluid closure which is beyond the scope of this paper. In general, we expect  $f_k < 1$ , and Ref. [22] suggests  $f_k \simeq 0.1$ . In this work, we use  $f_k = 0.1$  and 1 for a comparative study of the impact of  $f_K$  on the parallel energy loss. Main features presented in this paper, however, do not change by this  $f_K$  variation (except for the amount of parallel energy losses). We expect the actual value of  $f_K$  will be within this range.

Figures 5(a) and (b) show time evolution of instantaneous heat flux ( $Q$ ) and the cumulative ratio of the energy loss to the initial energy ( $\Delta W/W$ ) during simulations. Blue (red)



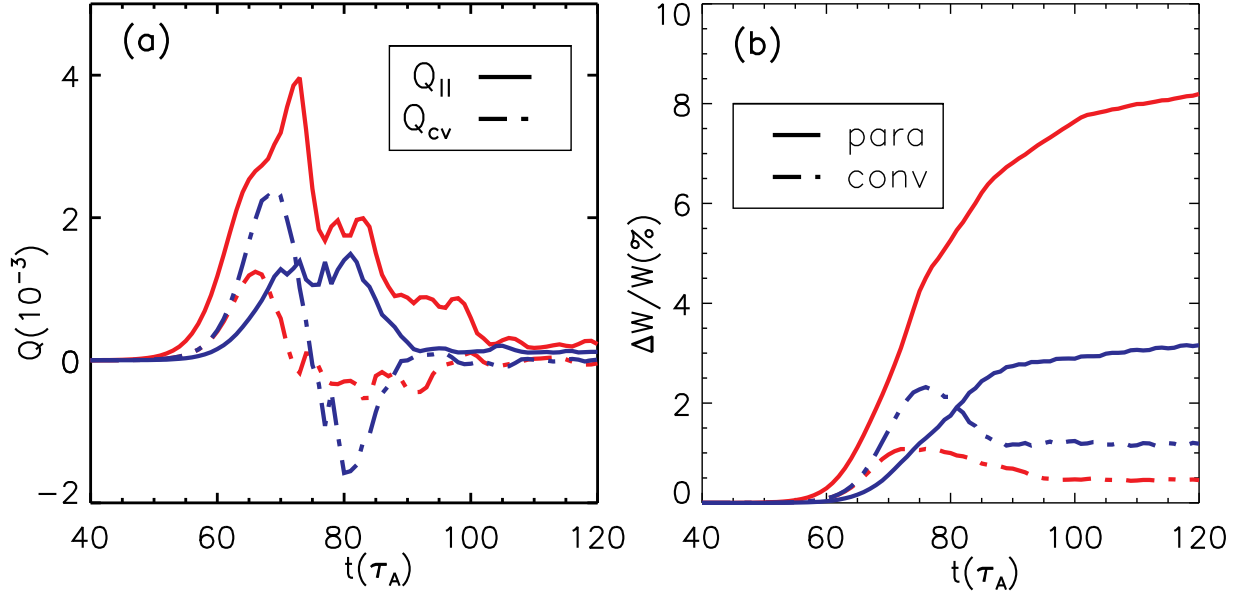


FIG. 5. Time evolution of (a) instantaneous heat flux ( $Q$ ) and (b) the cumulative ratio of ELM energy loss to the initial energy  $\Delta W/W$  during simulations. Blue (red) lines represents when  $f_K = 0.1$  ( $f_K = 1.0$ ). Dotted lines are  $Q$  and  $\Delta W/W$  due to the  $E \times B$  convection while solid lines represent those from  $Q_{||}$ .

lines represents the result when  $f_K = 0.1$  ( $f_K = 1.0$ ). Also, dotted lines are  $Q$  and  $\Delta W/W$  due to  $E \times B$  convection and solid lines represent those originated from  $Q_{||}$ . When  $f_K$  is small ( $=0.1$ ), the convective loss,  $Q_{cv}$ , is greater than  $Q_{||}$  in the early stage of a crash (*i.e.*, when  $60 \leq t \leq 80$ ). However,  $Q_{||}$  becomes dominant after  $t \simeq 80$ . Thus,  $Q_{||}$  is responsible for the majority of the net collapse-induced energy loss, taking up  $\sim 75\%$  of total  $\Delta W/W$ . When  $f_K$  is large ( $=1.0$ ),  $Q_{||}$  is always dominant over  $Q_{cv}$ , as shown in red lines in Figs. 5(a) and (b).

Now, we briefly discuss the role of hyper-resistivity ( $\eta_H$ ), which was highlighted in previous studies [14, 15], in relation to the field line stochastization.  $\eta_H$  represents electron dynamics in these simulations and may originate from, for instance, the residual electron temperature gradient turbulence in the edge pedestal [23]. We find that  $\eta_H$  plays two key roles in the pedestal collapse. First, it enhances the growth of STM by increasing the growth rate of PBM. Second, it increases the nonlinear growth of PTM, hence expediting the stochastization process. In this way, the increase of  $\eta_H$  shortens the ELM crash phase, whilst the decrease of it delays or even prohibits the pedestal collapse.

In summary, we found, from three-dimensional nonlinear simulations, that two important dynamical processes are involved in the edge pedestal collapse: (1) the generation of nonlinearly driven tearing modes from unstable ballooning modes and subsequent stochastization of magnetic fields, (2) the significant parallel energy loss through the stochastic lines. Based on these findings, we propose the ELM crash process as follows: (1) the generation of STMs through a nonlinear energy transfer between adjacent PBMs, (2) the generation of PTMs by extracting energy from a PBM *via* STMs, (3) island overlap, and eventual stochastization of magnetic field lines, and (4) a large energy loss through parallel conduction along the stochastic field lines.

The present study indicates the possible presence of a precursor period during which STMs develop from PBMs. Strong magnetic activities are then expected to be observed prior to an ELM crash with a toroidal mode number nearly twice as large as that of the original ballooning modes. In this sense, STMs might be a possible candidate for the precursor mode which has been observed in several experiments[10, 12, 24, 25]. As a future work, it is of importance to improve the model for  $Q_{\parallel}$  in the presence of stochastic field lines by developing a rigorous fluid closure model for it. Also, studying the impact of external resonant magnetic perturbations on the pedestal collapse scenario presented in this Letter is an immediate next step, which is under consideration.

The authors are grateful to Drs. P. H. Diamond and A. Aydemir for useful discussions. They also acknowledge to Drs. X. Q. Xu, A. Dimits, and M. Umansky for their help in the development of analysis codes using the BOUT++ framework. This work was supported by the WCI program of National Research Foundation of Korea funded by Ministry of Science, ICT and Future Planning of Korea [WCI 2009-001].

---

\* Corresponding author. hgjhang@nfri.re.kr

- [1] F. Wagner *et. al.*, Phys. Rev. Lett. **49**, 1408 (1982).
- [2] P. Snyder, H. Wilson, J. Ferron, L. Lao, A. Leonard, T. Osborne, A. Turnbull, D. Mossessian, M. Murakami, and X. Xu, Phys. Plasmas **9**, 2037 (2002).
- [3] G. T. A. Huysmans, S Pamela, E van der Plas, and P Ramet, Plasma Phys. Control. Fusion **51**, 124012 (2009).

- [4] B. Dudson, X. Q. Xu, M. V. Umansky, H. R. Wilson, and P. B. Snyder, *Plasma Phys. Control. Fusion* **53**, 054005 (2011).
- [5] L. E. Sugiyama and H. R. Strauss, *Phys. Plasmas* **17**, 062505 (2010).
- [6] A. Kirk *et. al.*, *Plasma Phys. Control. Fusion* **48**, B433 (2006).
- [7] B. Koch, A. Herrmann, A. Kirk, H. Meyer, J. Dowling, J. Harhausen, J. Neuhauser, H.W. Müller, W. Bohmeyer, G. Fussmann *et. al.*, *Jour. of Nucl. Mat.* **363-365**, 1056 (2007).
- [8] M. W. Jakubowski, W. Fundamenski, G. Arnoux, Th. Eich, R.A. Pitts, D. Reiter, R.C. Wolf, and JET-EFDA contributors, *Jour. of Nucl. Mat.* **390-391**, 781 (2009).
- [9] M. E. Fenstermacher, T. H. Osborne, A. W. Leonard, P. B. Snyder, D. M. Thomas, J.A. Boedo, T. A. Casper, R. J. Groebner, M. Groth, M. A. H. Kempenaars *et. al.*, *Nucl. Fusion* **45**, 1493 (2005).
- [10] G. S. Yun, W. Lee, M. J. Choi, J. Lee, H. K. Park, B. Tobias, C. W. Domier, N. C. Luhmann, Jr., A. J. H. Donne, and J. H. Lee, *Phys. Rev. Lett.* **107**, 045004 (2011).
- [11] H. R. Wilson and S. C. Cowley, *Phys. Rev. Lett* **92**, 175006 (2004).
- [12] A. Kirk, D. Dunai, M. Dunne, G. Huijsmans, S. Pamela, M. Becoulet, J.R. Harrison, J. Hillesheim, C. Roach, S. Saarelm, arXiv:1312.4300.
- [13] J. Peer, A. Kendl, and B. D. Scott, *Plasma Phys. Control. Fusion* **55**, 015002 (2013).
- [14] X. Q. Xu, B. Dudson, P. B. Snyder, M.V. Umansky, and H. Wilson, *Phys. Rev. Lett* **105**, 175005 (2010).
- [15] X. Q. Xu, B. D. Dudson, P. B. Snyder, M. V. Umansky, H. R. Wilson, and T. Casper, *Nucl. Fusion* **51**, 103040 (2011).
- [16] P.W. Xi, X. Q. Xu, and P. H. Diamond, *Phys. Rev. Lett.* **112**, 085001 (2014).
- [17] B. Dudson, M. Umansky, X. Xu, P. Snyder, and H. Wilson, *Comput. Phys. Commun.* **180**, 1467 (2009).
- [18] S. C. Cowley and M. Artun, *Phys. Rep.* **283**, 185 (1997).
- [19] B. V. Waddell, B. Carreras, H. R. Hicks and J. A. Holmes, *Phys. Fluids* **22**, 896 (1979). 185 (1997).
- [20] B. A. Carreras, M. N. Rosenbluth and H. R. Hicks, *Phys. Rev. Lett.* **46**, 1131 (1981).
- [21] A. B. Rechester and M.N. Rosenbluth, *Phys. Rev. Lett.* **40**, 38 (1978).
- [22] G. Park, C. S. Chang, I. Joseph, and R. A. Moyer, *Phys. Plasmas* **17**, 102503 (2010).
- [23] R. Singh, Hogun Jhang, and P. H. Diamond, *Phys. Plasmas* **20**, 112506 (2013).

[24] J. E. Boom *et. al.*, Nucl. Fusion **51**, 103039 (2011).

[25] Y. Sechrest, T. Munsat, D. J. Battaglia, and S.J. Zweben, Nucl. Fusion **52** 123009 (2012).